

Low-intensity, Kilohertz Frequency Spinal Cord Stimulation Differently Affects Excitatory and Inhibitory Neurons in the Rodent Superficial Dorsal Horn

Kwan Yeop Lee,^{a†} Chilman Bae,^{b†} Dongchul Lee,^a Zachary Kagan,^a Kerry Bradley,^a Jin Mo Chung^b and Jun-Ho La^{b*}

^a Nevro Corporation, Redwood City, CA, USA

^b Department of Neuroscience, Cell Biology, and Anatomy, University of Texas Medical Branch, Galveston, TX, USA

Abstract—Since 1967, spinal cord stimulation (SCS) has been used to manage chronic intractable pain of the trunk and limbs. Compared to traditional high-intensity, low-frequency (<100 Hz) SCS that is thought to produce paresthesia and pain relief by stimulating large myelinated fibers in the dorsal column (DC), low-intensity, high-frequency (10 kHz) SCS has demonstrated long-term pain relief without generation of paresthesia. To understand this paresthesia-free analgesic mechanism of 10 kHz SCS, we examined whether 10 kHz SCS at intensities below sensory thresholds would modulate spinal dorsal horn (DH) neuronal function in a neuron type-dependent manner. By using *in vivo* and *ex vivo* electrophysiological approaches, we found that low-intensity (sub-sensory threshold) 10 kHz SCS, but not 1 kHz or 5 kHz SCS, selectively activates inhibitory interneurons in the spinal DH. This study suggests that low-intensity 10 kHz SCS may inhibit pain sensory processing in the spinal DH by activating inhibitory interneurons without activating DC fibers, resulting in paresthesia-free pain relief. © 2020 The Authors. Published by Elsevier Ltd on behalf of IBRO. This is an open access article under the CC BY license (<http://creativecommons.org/licenses/by/4.0/>).

Key words: spinal cord stimulation, superficial dorsal horn neurons, high frequency, kilohertz.

INTRODUCTION

Since 1967, spinal cord stimulation (SCS), either at low (<100 Hz) or at high (>1.5 kHz) stimulation frequency, has been clinically used to manage chronic intractable pain of the trunk and limbs, but its pain-relieving mechanism(s) remain unclear (Shealy et al., 1967; Kumar et al., 2008; Foreman and Linderoth, 2012; Guan, 2012; Kapural et al., 2016; Crosby et al., 2017; Li et al., 2018). The analgesic mechanisms of low-frequency SCS have been investigated since the early 1970's and are generally based upon the Gate Control Theory of pain (Melzack and Wall, 1965). Although its definitive primary mechanism has not been determined yet, it is thought that large diameter A β fibers must be activated for low-frequency SCS to produce pain relief, and the degree of inhibition of dorsal horn (DH) wide-

dynamic range (WDR) neurons is positively correlated with stimulation intensity (Yang et al., 2014). This proposed mechanism has some clinical validation; it is known that paresthesia (defined as any abnormal sensation, caused by A β fiber activation, including what is often perceived by patients as tingling, buzzing, pins and needles, pressure, etc.) must be experienced by patients, and the body areas of paresthesia must overlap the patients' painful areas to result in pain relief (North et al., 1991; Oakley and Prager, 2002; Krames et al., 2008). This overlap is an ostensible indication of convergence of A β terminal projections to hyperexcitable regions of the DH (Smits et al., 2012).

However, this "A β fiber activation" seems unlikely to play a mechanistically significant role in the pain relief by high-frequency (e.g., 10 kHz) SCS. In contrast to low-frequency, paresthesia-based SCS, patients do not experience stimulation-induced abnormal sensations with low-intensity 10 kHz SCS, and the overlap between A β fiber-mediated paresthesia and painful areas targeted by 10 kHz SCS appears uncorrelated to pain relief (De Carolis et al., 2017). Recent *in vivo* work using rats demonstrated that low-intensity 10 kHz SCS significantly reduced the wind-up response of superficial spinothalamic tract neurons close to the SCS electrodes (McMahon et al., 2017). Since the stimulation intensities used in the study were too low to activate nearby large

*Corresponding author. Address: Department of Neuroscience, Cell Biology, and Anatomy, University of Texas Medical Branch, 301 University Boulevard, Galveston, TX 77555-1069, USA.

E-mail address: jula@UTMB.EDU (J.-H. La).

† These authors equally contributed to this work.

Abbreviations: AP, action potential; DC, dorsal column; DH, dorsal horn; EGTA, ethylene glycol-bis(β -aminoethyl ether)-N,N,N',N'-tetraacetic acid; GABA, gamma-aminobutyric acid; GFP, green fluorescent protein; HEPES, 4-(2-hydroxyethyl)-1-piperazineethanesulfonic acid; MT, motor threshold; NMDG, N-methyl-D-glucamine; SCS, spinal cord stimulation; VF, von Frey; WDR, wide-dynamic range.

myelinated A β fibers, it remains unknown how the SCS produced such inhibitory modulation of DH neuronal activity.

In the present work, therefore, we explored potential mechanisms for how 10 kHz SCS inhibits pain sensory processing in the spinal DH, by examining its effects on excitatory and inhibitory DH neurons. Performing *in vivo* electrophysiological experiments, we found that 10 kHz SCS at intensities below sensory thresholds preferentially activates putative inhibitory interneurons with no effect on putative excitatory interneurons, which was corroborated by *ex vivo* electrophysiological recordings of identified GABAergic inhibitory neurons in the DH.

EXPERIMENTAL PROCEDURES

All experimental procedures were carried out in accordance with the National Institute of Health Guide for the Care and Use of Laboratory Animals and approved by the Animal Care Committee at Vivocore Resources Inc and the Institutional Animal Care and Use Committee at the University of Texas Medical Branch. All efforts were made to minimize the number of animals used and their suffering in this study.

Animal preparation for *in vivo* experiments

In vivo experiments were performed on adult male Sprague Dawley rats obtained from Charles River, Montreal. A total of 12 rats was used for this study. Under urethane anesthesia (20% in saline; 1.2 g/kg, intraperitoneally), a laminectomy was performed to expose L4–S1 segments of the spinal cord. The rat was then placed in a stereotaxic frame, and its vertebrae were clamped above and below the recording site to immobilize the spinal cord. The left hind paw was immobilized in plasticine with the plantar surface facing upwards to receive mechanical stimuli. Rectal temperature was kept at 37 °C using a feedback-controlled heating pad (TR-200; Fine Science Tools, Taunton, MA) throughout the experiment.

Single unit extracellular recordings

A 4-shank probe with a total of 16 recording microelectrodes (A4x4-3mm-50-125-177-A16, NeuroNexus) was implanted at the L5 spinal level in the left DH. The array was oriented parallel to the rostrocaudal axis so that each electrode was at roughly the same mediolateral position. Depth of electrode insertion was monitored to estimate electrode position within presumed Rexed lamina(e). Electrode shank tips were lowered $354 \pm 87 \mu\text{m}$ (mean \pm standard deviation) below the dorsal surface. Since recording sites are spaced at 50 μm intervals up each shank of the electrode, we estimated the depth of recorded neurons to be positioned within lamina I or II. Neurons that responded to limb displacement, indicating that they received proprioceptive input, were excluded. Measured extracellular signals of neuronal activity were amplified, band-pass filtered between 500 Hz and 10 kHz, digitized at 40 kHz with OmniPlex Data Acquisition System

(Plexon, Dallas, TX, USA), and stored with stimulus markers on disk. Single units were isolated using Offline Sorter v3 software (Plexon) and were analyzed with NeuroExplorer 4 (Plexon).

Mechanical stimulation

Cutaneous receptive fields were identified on the basis of observed spiking evoked by mechanical stimuli applied using a brush or von Frey (VF) filaments to the glabrous skin of the left hind paw. By using weak search stimuli (to avoid peripheral sensitization), we specifically targeted neurons receiving low-threshold afferent input. Each stimulus comprised 10 one-second-long applications of the brush or VF filament (2, 4, 6, 8, and 10 g) repeated at 2-s intervals. Each stimulus was applied twice onto different locations within the receptive field for each test condition.

SCS

SCS was applied via a miniature in-line quadripolar electrode array (420 μm diameter, 1 mm-long contact leads interspaced with 1.5 mm-long nonconductive polymers), positioned epidurally over the L5–L6 dorsal spinal segments (innervating the left hind paw). The SCS electrode was medially positioned within 1–2 mm of the recording microelectrode probe. Two contacts on the miniature SCS lead were used to provide bipolar stimulation, delivered from a modified version of the same trial stimulator used clinically for 10 kHz SCS therapy (Trial Stimulator, Nevro, Redwood City, USA). Stimulation was delivered as a continuous train of symmetric, biphasic, 30 μs -per-phase pulses, at a variety of kHz frequencies and pulse amplitudes (see ‘Protocol’). Initially, to determine the motor threshold (MT), stimulation at each tested frequency was gradually increased until motor twitch (most often in the hindpaw, but also observed in the paraspinal musculature/trunk). To allow for clear visualization of muscle activity, the stimulation was duty cycled at 300-ms ON, and 2-s OFF.

General protocol

After insertion of the recording microelectrode probe, mechanical stimuli were applied to the hindpaw to determine neurons responsive to innocuous brush stimuli and strong VF (10 g). Next, SCS was applied at 1 kHz, 5 kHz, and 10 kHz, at intensities of 10% and 30% of MT, which are reportedly below the sensory threshold (Song et al., 2014), as well as at 60% and 90% MT, while neuronal response was recorded (Fig. 1). SCS was then administered for periods of 40 s at each stimulation setting while DH neuronal response was recorded. SCS was left OFF for at least 5 min between measurement periods.

Patch-clamp recording of DH neurons in *ex vivo* spinal cord slices

Transgenic mice expressing green fluorescent protein (GFP) in GABAergic neurons (FVB-Tg(GadGFP))

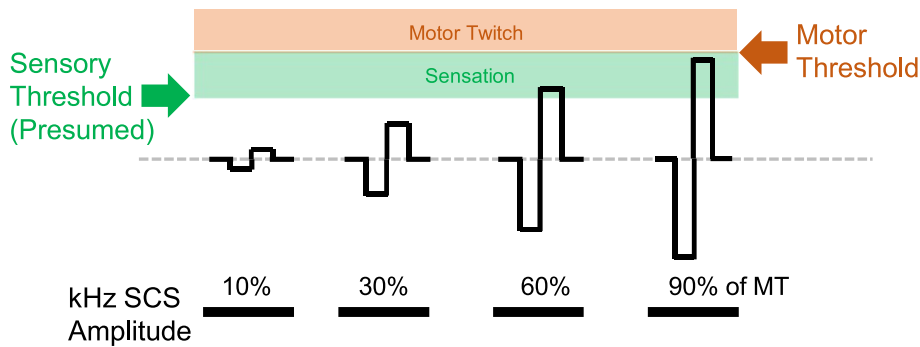


Fig. 1. Range of high-frequency (kHz) spinal cord stimulation (SCS) intensities applied in this study. Previous reports have suggested that SCS administered at intensities of 40–60% of motor threshold (MT) correlates to the clinical paresthesia onset threshold (Song et al., 2014). By testing the entire range of SCS intensity over multiple frequencies, the effects of frequency and amplitude can be independently assessed.

45704Swn/J, 4–6 weeks old, both sexes, produced in-house from breeders purchased from The Jackson Laboratory, Bar Harbor, ME) were used for *ex vivo* experiments. A total of five mice (three males, two females) was used for this study.

Spinal cord slices were prepared as previously described (Bae et al., 2018). Briefly, the spinal cord was sliced transversely at a thickness of 400 μm using a vibratome (Leica VT1200S, Buffalo Grove, IL, USA) in cold ($\sim 4^{\circ}\text{C}$) NMDG (N-methyl-D-glucamine) solution (in mM: 93 NMDG, 2.5 KCl, 1.2 NaH_2PO_4 , 30 NaHCO_3 , 20 HEPES, 25 glucose, 5 sodium ascorbate, 2 thiourea, 3 sodium pyruvate, 10 MgSO_4 and 0.5 CaCl_2 , pH 7.4) saturated with 95% O_2 and 5% CO_2 . Whole-cell recordings were made on GFP-positive (GFP(+)) or -negative (GFP(-)) neurons in lamina II in artificial cerebrospinal fluid (in mM: 124 NaCl, 2.5 KCl, 1.2 NaH_2PO_4 , 24 NaHCO_3 , 5 HEPES, 12.5 glucose, 2 MgSO_4 , and 2 CaCl_2 , pH 7.4) using MultiClamp 700B amplifier (Molecular Devices, Sunnyvale, CA, USA), Digidata (Molecular Devices) and pClamp software (version 10.6, Molecular Devices) at a 50 kHz sampling rate. The patch-pipettes (4–8 $\text{M}\Omega$) were filled with internal solution (in mM: 120 K-gluconate, 10 KCl, 2 Mg-ATP, 0.5 Na-GTP, 0.5 EGTA, 20 HEPES, and 10 phosphocreatine, pH 7.3). The neurons were further characterized by their action potential (AP)-firing pattern upon depolarizing current injections in the current clamp mode.

For 10 kHz SCS *ex vivo*, a miniature SCS electrode array was placed dorsal to the DC (Fig. 4) with its first lead being 0.1-mm distanced from the DC by an attached nonconductive polymer spacer. SCS, 30 μs -per-phase biphasic pulses at 10 kHz, was delivered for 300 ms at 2-s intervals and stimulation intensities ranging from 2 mA to 8 mA (2-mA step).

Data analysis

Data are expressed as mean \pm standard error of the mean (SEM) with n , the number of cells and N , the number of animals. For the *in vivo* experiments, to quantify and characterize the spiking evoked by mechanical stimulation of the hindpaw and by SCS, we

measured the mean firing rate of individual neurons during each stimulus, and subtracted the spontaneous firing rate measured from the 10-s epoch preceding each stimulus. As we sampled multiple neurons from a single animal (i.e., nested design), we performed multilevel analysis (Aarts et al., 2014) using a linear mixed model. Statistically analyzing the difference in cellular location or spontaneous firing rates between two cell types, we considered cell type a fixed categorical factor and individual rats a higher level random factor. When firing rates during SCS were analyzed, SCS intensity (% MT), SCS frequency, and their interaction were considered fixed categorical factors, while rats and the cells (nested within rats) were regarded as random categorical factors; the SCS intensity was a repeated variable.

In *ex vivo* experiments, the mean number of APs discharged during the 300-ms SCS was measured after applying an offline 1 kHz low-pass filter. Similar to the statistical analysis used for *in vivo* results, we performed multilevel analysis: we regarded SCS intensity (mA), neuron types (e.g., GFP(+/-) or AP firing-types), and their interaction as fixed categorical factors, and mice and the neurons (nested within mice) as random categorical factors; the SCS intensity was a repeated variable. In case that no significant interaction between SCS intensity and neuron types was detected (results for Fig. 5), the dataset was re-analyzed using a statistical model without interaction.

When statistically analyzing firing rates or AP numbers, despite our understanding that the F -test is robust in terms of Type I error even if the normality assumption is violated (Blanca et al., 2017), we took a conservative approach to meet both the normality and equal variance assumptions by transforming our data of AP firing (\log_e transformation; 0.01 was added to raw values to make all > 0 before the transformation). Differences between multiple groups with Bonferroni-adjusted $p \leq 0.05$ (e.g., unadjusted $p \leq 0.016$ for three comparisons in Figs. 3 and 5) were considered significant.

RESULTS

Spinal DH neurons recorded *in vivo* fall into two distinct groups: adapting and non-adapting neurons

Examining the effect of SCS on DH excitatory and inhibitory neurons separately is crucial, as simultaneous activation of these neurons might cancel each other's influence on pain processing and thus produce no apparent aggregate outcome. Therefore, as in Fig. 2, we classified the neurons recorded *in vivo* as excitatory and inhibitory cells based on criteria previously reported (Yasaka et al., 2010; Dougherty and Chen, 2016; Abreira et al., 2017). Specifically, neurons were identified

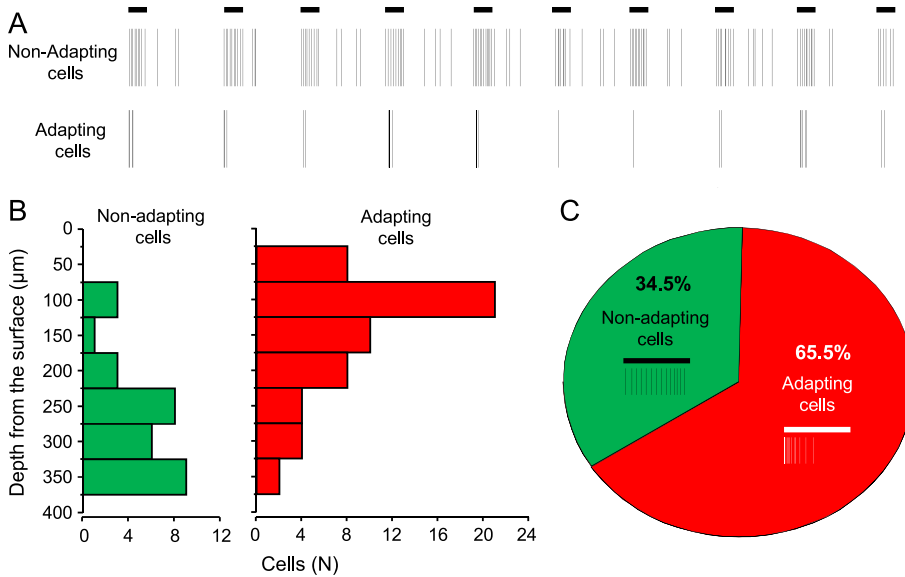


Fig. 2. Superficial dorsal horn (DH) neurons of the rat, extracellularly-recorded *in vivo*, are classified into two groups. **(A)** Representative Raster plots of two types of DH neurons, showing their distinct responses to von Frey filament (VF) stimulations (10 g for 1 s, indicated by horizontal black bars). Non-adapting cells continuously fire action potentials (APs) during the VF stimulation, whereas adapting cells cease AP firing during the stimulation. **(B)** Distribution of the depth of recorded neurons from the surface. **(C)** Proportion of the two neuronal groups (total $n = 87$).

and ‘adapting’ cells based on their responses to VF (10 g) stimulation (Fig. 2A). Next, we investigated the distribution of recording depths for all adapting ($n = 57$, $N = 10$) and non-adapting ($n = 30$, $N = 12$) neurons (Fig. 2B). Average depth for non-adapting cells ($267 \pm 14 \mu\text{m}$) was greater than that for adapting cells ($149 \pm 11 \mu\text{m}$, $F(1,86.9) = 46.1$, $p \leq 0.001$). Also, the proportion of adapting (65.5%) and non-adapting cells (34.5%) was about expected 2:1 ratio for excitatory and inhibitory interneurons in superficial laminae (Polgar et al., 2003; Todd, 2010, 2017) (Fig. 2C). The spontaneous firing rate of non-adapting cells (6.75 ± 0.99 , $n = 30$, $N = 12$) was higher than that of adapting cells (0.41 ± 0.08 , $n = 57$, $N = 10$; $F(1,86.9) = 60.8$, $p \leq 0.001$ using \log_e transformed data). In addition, more non-adapting cells (93%, 28 out of 30, $N = 12$) spontaneously fired APs than adapting cells

(61%, 35 out of 57, $p \leq 0.005$ by Fisher’s exact test). Based on the depth of recordings, we determined that the measured neurons were located within the superficial DH. Collectively, these data suggest that we sampled two distinct populations of superficial DH neurons, presumably excitatory (adapting cells) and inhibitory (non-adapting cells) subtypes as shown previously (Lee and Prescott, 2014; Lee et al., 2019). Furthermore, the relative distribution of these two cell types across the DH laminae (Fig. 2B) is consistent with the increasing proportion of inhibitory neurons from lamina I to III (Polgar et al., 2013).

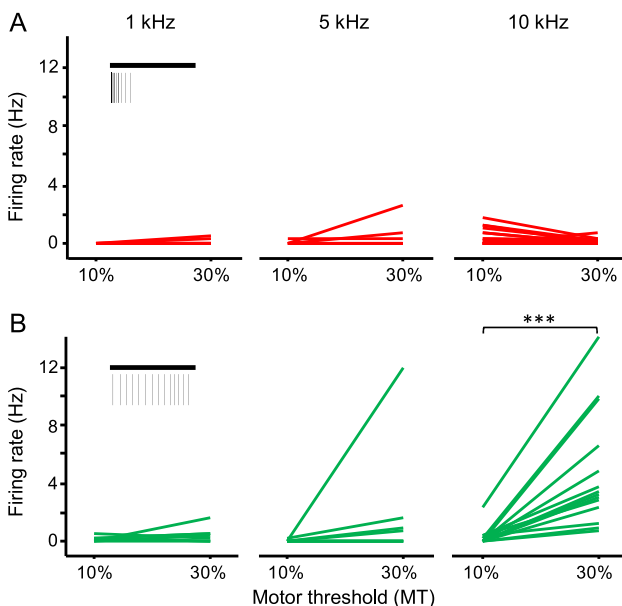


Fig. 3. Frequency- and intensity-dependent activation of adapting and non-adapting cells by SCS in superficial dorsal horn (DH) of the rat. Firing rates of adapting cells **(A)** 1 kHz: $n = 11$, 5 kHz: $n = 7$, 10 kHz: $n = 18$ and non-adapting cells **(B)** 1 kHz: $n = 8$, 5 kHz: $n = 8$, 10 kHz: $n = 14$ during SCS at 10% and 30% of motor threshold (MT) intensities. ***Adjusted $p \leq 0.001$ vs. firing rates at 10% MT by Bonferroni multiple comparison test following multilevel analysis using \log_e transformed data.

10 kHz SCS specifically activates non-adapting cells at 30% MT

In order to determine whether 10 kHz SCS has any effect on spinal DH neurons at stimulation intensities below sensory thresholds, we applied SCS at 10% and 30% of MT intensities (Fig. 3). 10 kHz SCS at 10% of MT did not substantially increase firing rates in adapting (0.50 ± 0.14 spike/s after subtracting spontaneous firing rates, $n = 18$, $N = 5$) and non-adapting cells (0.25 ± 0.16 spike/s after subtracting spontaneous firing rates, $n = 14$, $N = 5$). However, at 30% of MT, firing rates of non-adapting cells increased to 4.7 ± 1.1 spike/s ($n = 14$, $N = 5$; $t(46.3) = 7.43$, adjusted $p \leq 0.001$ vs. 10% MT using \log_e transformed data) during 10 kHz SCS, whereas those of adapting cells did not (0.16 ± 0.05 spike/s, $n = 18$, $N = 5$; $t(58.7) = 0.86$, adjusted $p > 0.39$ vs. 10% MT using \log_e transformed data). The firing rates in non-adapting cells during 10 kHz SCS at 30% of MT were $80 \pm 30\%$ ($n = 14$, $N = 5$) of brush-evoked responses, suggesting that 10 kHz SCS at sub-

by their AP firing pattern to 10-g VF filament stimulation, depth from the surface, and existence of spontaneous firing. We first identified the neuronal type as ‘non-adapting’

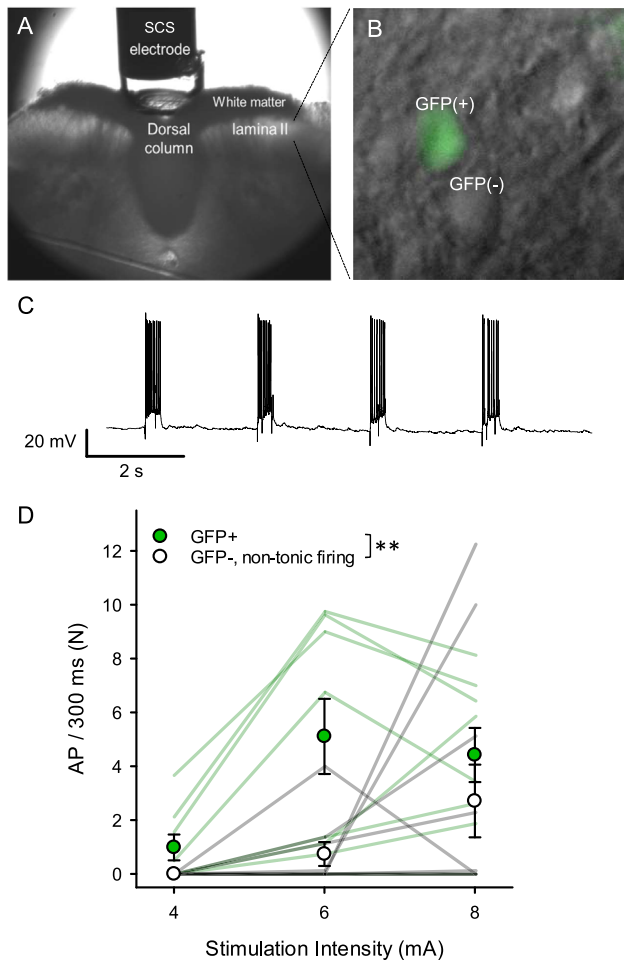


Fig. 4. Preferential activation of GABAergic inhibitory neurons over excitatory neurons by 10 kHz SCS in *ex vivo* spinal cord slices of the mouse. **(A)** Experimental configuration for SCS stimulation *ex vivo*. **(B)** patch-clamp recording of GABAergic inhibitory neuron identified by its GFP expression (GFP(+)) in the dorsal horn. **(C)** A representative trace showing GFP(+) GABAergic neuronal activation by 10 kHz SCS delivered for 300 ms at 2-s intervals. **(D)** The number of action potentials (APs) discharged during the 300-ms SCS at different intensities (4–8 mA). Note that GFP(+) neurons ($n = 8–9$, $N = 4$; not all neurons were tested across all stimulation intensities) fired more APs than GFP(-) neurons that were non-tonic-firing upon depolarizing current injections ($n = 7–11$, $N = 3$). ** $p \leq 0.01$ vs. GFP(-) neurons following multilevel analysis using \log_e transformed data.

sensory threshold intensity is as effective as A β fiber-mediated sensory inputs in activating DH inhibitory interneurons. Unlike 10 kHz SCS, however, 1 kHz (0.39 ± 0.18 spike/s after subtracting spontaneous firing rates, $n = 8$, $N = 4$) and 5 kHz SCS at 30% of MT (1.88 ± 1.45 spike/s after subtracting spontaneous firing rates, $n = 8$, $N = 4$) did not significantly increase the firing rates in non-adapting cells, compared with those at 10% of MT (at 1 kHz, $t(46.3) = 0.83$, unadjusted $p > 0.41$; at 5 kHz, $t(46.3) = 2.32$, adjusted $p > 0.07$ using \log_e transformed data).

When we applied 10 kHz SCS at 60% and 90% of MT intensities, which are likely above sensory threshold, adapting cells ($n = 18$, $N = 5$) fired 6.3 ± 2.1 and 12.9 ± 3.8 spikes/s at 60% and 90% MT after subtracting

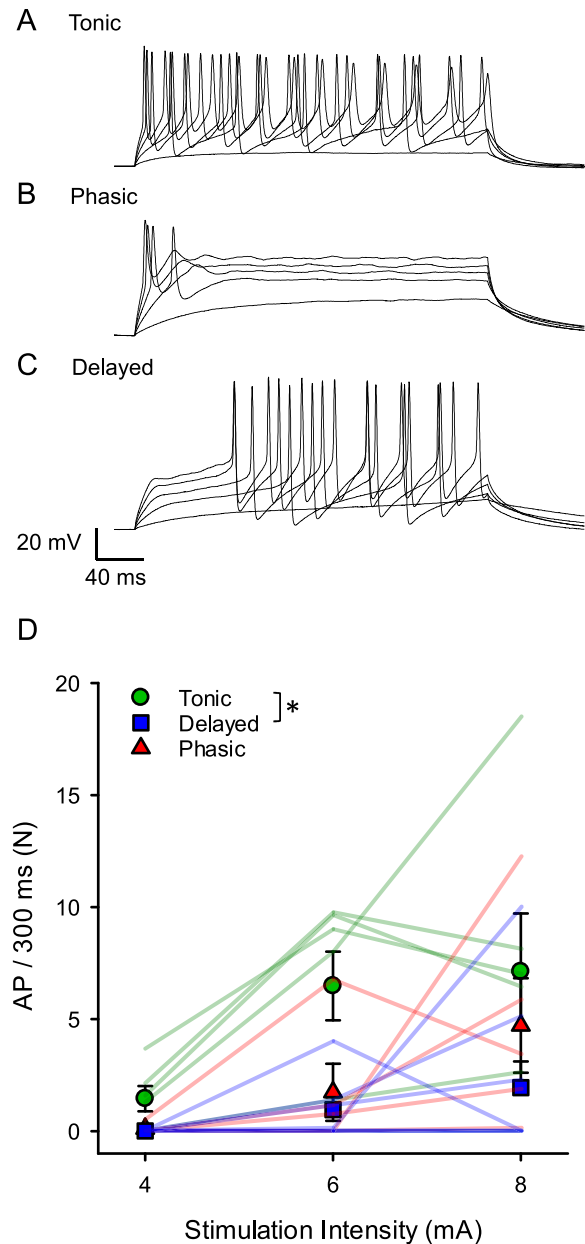


Fig. 5. Neuron type-dependent differential activation by 10 kHz SCS in *ex vivo* spinal cord slices of the mouse. **(A–C)** Representative traces showing three neuron types in the dorsal horn based on their action potential (AP) firing pattern upon depolarizing current injections. **(D)** Activation of the three neuron types by 10 kHz SCS. Tonic-firing neurons ($n = 6–7$, $N = 4$; not all neurons were tested across all stimulation intensities) were more readily activated by the SCS than delayed-firing neurons ($n = 6–9$, $N = 3$). No significant difference in AP numbers was detected between tonic- and phasic-firing neurons across the range of 4–8 mA SCS intensities when \log_e transformed data were used for statistical analysis. *Adjusted $p \leq 0.05$ vs. delayed-firing neurons by Bonferroni multiple comparison test following multilevel analysis using \log_e transformed data.

baseline firing rates, respectively; and non-adapting cells ($n = 14$, $N = 5$) 17.6 ± 5.9 and 36.4 ± 9.1 spikes/s. Together, these data suggest that 10 kHz SCS, but not 1 kHz or 5 kHz SCS, is able to activate non-adapting, putative inhibitory interneurons at sub-sensory threshold levels of stimulation intensity (i.e., 30% MT)

without activating adapting, presumed excitatory interneurons. However, when SCS intensity is at supra-sensory threshold, such differential activation between the two neuron types is no longer attained.

Preferential activation of GABAergic inhibitory neurons by 10 kHz SCS in spinal cord slices *ex vivo*

To validate the above *in vivo* findings, namely the preferential activation of putative inhibitory interneurons over excitatory neurons by 10 kHz SCS, we performed patch-clamp recordings using *ex vivo* spinal cord slices prepared from transgenic mice whose GFP expression is driven by Gad67 promoter activity (Oliva et al., 2000). The majority (62–75%) of GFP(+) GABAergic neurons in these transgenic mice were previously shown to be tonic-firing (i.e., non-adapting) upon depolarizing current injection (Daniele and MacDermott, 2009), whereas excitatory neurons in the DH are single-, phasic-, or delayed-firing (Punnakkal et al., 2014).

In response to 10 kHz SCS at 2 mA, only 1 of 9 GFP(+) GABAergic neuron ($N = 4$) fired APs; none of 7 non-tonic firing GFP(–) neurons ($N = 3$), presumably excitatory neurons, fired APs. In the range of 4–8 mA SCS intensities, GFP(+) neurons ($n = 8–9$, $N = 4$; not all neurons were tested across all stimulation intensities) fired more APs than presumed excitatory interneurons ($n = 7–11$, $N = 3$) (Fig. 4; $F(1,17.3) = 12.18$, $p \leq 0.01$ using \log_e transformed data). At 8 mA stimulation, only 1 of 8 GFP(+) neurons failed to fire AP, whereas about a half (5 of 11) of non-tonic firing GFP(–) neurons did. Such differential neuronal activation by 10 kHz SCS was also evident when neurons were classified into tonic-, phasic-, and delayed-firing neurons solely by their AP firing patterns upon depolarizing current injection. As shown in Fig. 5, 10 kHz SCS more readily activated tonic-firing neurons ($n = 6–7$, $N = 4$) than delayed-firing ($n = 6–9$, $N = 3$) neurons ($F(2,16.8) = 5.21$, $p \leq 0.05$ between the 3 neuronal types; $t(18.1) = 3.26$, adjusted $p \leq 0.05$ between tonic- vs. delayed-firing neurons; $t(15.5) = 1.51$, adjusted $p > 0.45$ between tonic- vs. phasic-firing neurons using \log_e transformed data). At 8 mA stimulation, 1 of 6 tonic-firing neurons, 0 of 5 phasic-firing neurons, and 6 of 9 delayed-firing neurons failed to fire AP.

DISCUSSION

Traditional low-frequency SCS has been assumed to rely upon the activation of the large myelinated axon projections of A β fibers in the dorsal column (DC) (Oakley and Prager, 2002). Clinically, this results in paresthesia, likely from the SCS-induced activity in the DC pathway travelling orthodromically through the DC nuclei, the thalamus, and ultimately driving perception upon reaching the cortex. Still, the majority of preclinical work suggests that the pain-relieving effects of SCS are segmental, due to the APs delivered to the DH of hyper-excitable spinal segments via collateral projections of those same DC fibers (Yowtak et al., 2011). Preclinical studies have shown that the higher the stimulation amplitude, the more apparent the inhibitory effects, while much

less effect is observed at stimulation amplitudes believed to be below the DC fiber activation threshold (Shechter et al., 2013; Yang et al., 2014). The translational relationship between preclinical stimulation intensity levels, clinical paresthesia and MT has not, to our knowledge, been determined in a systematic or definitive way. Like other investigators, we used the MT as an upper limit on clinically relevant stimulation intensity (Russo et al., 2018). Previous reports suggested that SCS administered at intensities of 40–60% of MT correlate to the clinical paresthesia onset threshold, likely from the activation of DC fibers (Song et al., 2014). Thus, we assumed that stimulation intensities of no greater than 30% of MT would translate to ‘paresthesia-free’ clinical settings not activating DC fibers. In this study, we observed that 10 kHz SCS is capable of selectively driving inhibitory interneurons in the superficial DH at 30% of MT, whereas it activates both excitatory and inhibitory DH neurons at 60% and 90% MT. Therefore, low-intensity 10 kHz SCS may be able to modulate inhibitory interneurons (and thus relieve pain) without triggering spinal nociceptive circuit activation and interrupting somatosensory mechanisms mediated by excitatory neurons in the spinal DH. We acknowledge that classifying excitatory and inhibitory cells *in vivo* based on extracellular recordings of firing, locational, and proportional properties as described in this study is not definitive although such classification system has been previously utilized (Lee and Prescott, 2014; Lee et al., 2019). Therefore, as a corroborative approach, we identified inhibitory and excitatory neurons in *ex vivo* spinal cord slices based on GFP-expression and tonic-firing pattern and compared their responses to a range of SCS intensities with those of their counterparts. The *ex vivo* study showed that stimulation-response profiles of identified GFP(+) GABAergic neurons or tonic-firing neurons were left-shifted, compared to those of GFP(–) neurons or phasic/delayed-firing neurons, supporting the *in vivo* findings that low-intensity 10 kHz SCS preferentially activates spinal inhibitory neurons over their excitatory counterparts. The mechanistic basis of this neuron type-dependent effect of low-intensity 10 kHz SCS is currently unclear, and investigation of such mechanisms is beyond the scope of present work. It would be of interest in future study to examine the nature of SCS-responsive apparatus in the DH neurons and functional/expressional difference of the apparatus between inhibitory and excitatory neurons. As it is also possible that activation of excitatory neurons by low-intensity 10 kHz SCS is hampered by simultaneous, robust activation of inhibitory interneurons in the DH neural network, it will be necessary in future study to assess the contribution of local inhibitory neurotransmission to the neuron type-dependent effect of low-intensity 10 kHz SCS.

We found frequency to be a critical factor for selective activation of DH neurons. At low intensities, SCS using 10 kHz, not 1 kHz or 5 kHz, could solely activate non-adapting inhibitory neurons. It may be that certain channels that predominate on DH neuronal membranes are sensitive to the repetition rate of pulse delivery. Temporal summation is a well-known phenomenon of synaptic transmission, where more rapid release of

neurotransmitter increases the likelihood of post-synaptic cell firing (Kandel et al., 2000). Non-synaptic neural membranes also appear to demonstrate a form of temporal summation, where the effect is mediated by non-synaptic mechanisms. Bromm (1975) demonstrated that frequencies greater than approximately 4 kHz could repetitively activate sodium channels to the point of AP generation. Reilly et al. (1985) used computational modeling of mammalian axons to demonstrate that reduced stimulation pulse amplitudes could still generate APs if >5 kHz sinusoidal frequencies were used. Similarly, Schoen and Fromherz (2008) used weak capacitive currents administered at >1.5 kHz to repetitively activate Nav1.4 channels in rat neurons, and ultimately generate APs. In our experiments, if SCS-induced AP firings below sensory threshold intensity were triggered by temporal summation of cation channel-mediated small depolarization, the summated depolarization must be able to reach AP threshold only in inhibitory neurons at 10 kHz.

In performing our *in vivo* experiments, we placed recording electrodes only in the local DH. We did not measure more rostral activity (e.g., cord dorsum potentials, gracile nuclei activity, etc.), so we do not know the actual stimulation amplitude range that activates DC fibers. Thus, we do not know precisely which observed effects may be influenced by synaptic drive from activated DC collaterals. The same limitation also applies to our data obtained from *ex vivo* spinal cord slices. Still, our assumption that stimulation amplitudes $\leq 30\%$ of MT would not activate DC axons is in keeping with most prior preclinical literature. In addition, it is noteworthy that in *ex vivo* spinal cord slices prepared from the same transgenic mouse strain in a similar fashion, A β fiber input-evoked activation of GABAergic neurons was seldom observed presumably due to damages in the incoming A β fibers along their DC passage (Schoffnegger et al., 2006; Daniele and MacDermott, 2009). Therefore, it could be that in our *ex vivo* experiments, contribution of DC collaterals to SCS-induced GABAergic neuronal activation is physically limited.

Without measurement of neuronal response to antidromic stimulation at supraspinal sites in our experiments, we cannot determine whether the DH neurons we measured were local interneurons or projection neurons. We presume that, given that projection neurons are absent in lamina II and represent only up to 5% of neurons in the lumbar segments of lamina I in the rat (Spike et al., 2003), it is likely that the majority of neurons we studied were local interneurons, about 1/3 of which are inhibitory and the remainder are excitatory (Todd, 2017).

Our experiments were in anesthetized animals, and stimulation was only applied for seconds–minutes. Thus, what we measured are acute, rapid onset electrophysiological effects. It has been observed clinically that pain relief onset from 10 kHz SCS can typically be appreciated hours to days after starting SCS. Thus, we speculate that our measurements relate to the start of a cascade of changes that may ultimately result in perceivable pain relief. Study of these effects in

longer-term models, including behavioral assays would be valuable to truly assess mechanisms for pain relief by low-intensity 10 kHz SCS.

In conclusion, by using *in vivo* and *ex vivo* electrophysiological approaches, we found that low-intensity 10 kHz SCS, but not 1 kHz or 5 kHz SCS, selectively activates inhibitory interneurons in the spinal DH. This study suggests that low-intensity 10 kHz SCS may inhibit pain sensory processing in the spinal DH by activating inhibitory interneurons without activating DC fibers, ultimately resulting in paresthesia-free pain relief.

ACKNOWLEDGEMENTS

Research conducted at UTMB was funded by Nevro Corp.

We thank Jean-Louis Marchal for statistical analysis of the results of this study.

DECLARATION OF INTEREST

Lee KY: Nevro Corp employee.

Bae C: Research support from Nevro Corp.

Lee D: Nevro Corp employee.

Kagan Z: Nevro Corp employee.

Bradley L: Nevro Corp employee.

Chung JM: No conflict of interest.

La JH: Research support from Nevro Corp.

REFERENCES

- Aarts E, Verhage M, Veenvliet JV, Dolan CV, van der Sluis S (2014) A solution to dependency: using multilevel analysis to accommodate nested data. *Nat Neurosci* 17:491–496.
- Abraira VE et al (2017) The cellular and synaptic architecture of the mechanosensory dorsal horn. *Cell* 168. 295–310 e219.
- Bae C, Wang J, Shim HS, Tang SJ, Chung JM, La JH (2018) Mitochondrial superoxide increases excitatory synaptic strength in spinal dorsal horn neurons of neuropathic mice. *Mol Pain* 14. 1744806918797032.
- Blanca MJ, Alarcón R, Arnau J, Bono R, Bendayan R (2017) Non-normal data: is ANOVA still a valid option? *Psicothema* 29:552–557.
- Bromm B (1975) Spike frequency of the nodal membrane generated by high-frequency alternating current. *Pflügers Arch* 353:1–19.
- Crosby ND, Janik JJ, Grill WM (2017) Modulation of activity and conduction in single dorsal column axons by kilohertz-frequency spinal cord stimulation. *J Neurophysiol* 117:136–147.
- Daniele CA, MacDermott AB (2009) Low-threshold primary afferent drive onto GABAergic interneurons in the superficial dorsal horn of the mouse. *J Neurosci* 29:686–695.
- De Carolis G, Paroli M, Tollapi L, Doust MW, Burgher AH, Yu C, Yang T, Morgan DM, Amirdelfan K, Kapural L, Sitzman BT, Bundschu R, Vallejo R, Benyamin RM, Yearwood TL, Gliner BE, Powell AA, Bradley K (2017) Paresthesia-independence: an assessment of technical factors related to 10 kHz paresthesia-free spinal cord stimulation. *Pain Phys* 20:331–341.
- Dougherty PM, Chen J (2016) Relationship of membrane properties, spike burst responses, laminar location, and functional class of dorsal horn neurons recorded in vitro. *J Neurophysiol* 116:1137–1151.
- Foreman RD, Linderth B (2012) Neural mechanisms of spinal cord stimulation. *Int Rev Neurobiol* 107:87–119.
- Guan Y (2012) Spinal cord stimulation: neurophysiological and neurochemical mechanisms of action. *Curr Pain Headache Rep* 16:217–225.

- Kandel ER, Schwartz JH, Jessell TM (2000) Principles of neural science. New York: McGraw-Hill.
- Kapural L, Yu C, Doust MW, Gliner BE, Vallejo R, Sitzman BT, Amirdelfan K, Morgan DM, Yearwood TL, Bundschu R, Yang T, Benjamin R, Burgher AH (2016) Comparison of 10-kHz high-frequency and traditional low-frequency spinal cord stimulation for the treatment of chronic back and leg pain: 24-month results from a multicenter, randomized, controlled pivotal trial. *Neurosurgery* 79:667–677.
- Krames ES, Oakley JC, Foster AM, Henderson J, Prager JP, Rashbaum RR, Stamos J, Weiner RL (2008) Spinal cord stimulation has comparable efficacy in common pain etiologies. *Neuromodulation* 11:171–181.
- Kumar K, Taylor RS, Jacques L, Eldabe S, Meglio M, Molet J, Thomson S, O'Callaghan J, Eisenberg E, Milbouw G, Buchser E, Fortini G, Richardson J, North RB (2008) The effects of spinal cord stimulation in neuropathic pain are sustained: a 24-month follow-up of the prospective randomized controlled multicenter trial of the effectiveness of spinal cord stimulation. *Neurosurgery* 63:762–770. discussion 770.
- Lee KY, Prescott SA (2014) Impact of spinal interneuron disinhibition on somatosensory processing in neuropathic pain 2014 Neuroscience Meeting Planner: Program No. 627.617/GG624.
- Lee KY, Ratté S, Prescott SA (2019) Excitatory neurons are more disinhibited than inhibitory neurons by chloride dysregulation in the spinal dorsal horn. *eLife* 8.
- Li S, Farber JP, Linderth B, Chen J, Foreman RD (2018) Spinal cord stimulation with “conventional clinical” and higher frequencies on activity and responses of spinal neurons to noxious stimuli: an animal study. *Neuromodulation* 21:440–447.
- McMahon S, Smith T, Lee D, Bradley K (2017) Electrophysiological investigation of the effects of 10 kHz spinal cord stimulation on the excitability of superficial dorsal horn neurons in experimental pain models. *Neuromodulation: Technology at the Neural Interface* 20:e678.
- Melzack R, Wall PD (1965) Pain mechanisms: a new theory. *Science* 150:971–979.
- North RB, Ewend MG, Lawton MT, Piantadosi S (1991) Spinal cord stimulation for chronic, intractable pain: superiority of “multi-channel” devices. *Pain* 44:119–130.
- Oakley JC, Prager JP (2002) Spinal cord stimulation: mechanisms of action. *Spine (Phila Pa 1976)* 27:2574–2583.
- Oliva AA, Jiang M, Lam T, Smith KL, Swann JW (2000) Novel hippocampal interneuronal subtypes identified using transgenic mice that express green fluorescent protein in GABAergic interneurons. *J Neurosci* 20:3354–3368.
- Polgar E, Durieux C, Hughes DI, Todd AJ (2013) A quantitative study of inhibitory interneurons in laminae I–III of the mouse spinal dorsal horn. *PLoS One* 8 e78309.
- Polgar E, Hughes DI, Riddell JS, Maxwell DJ, Puskar Z, Todd AJ (2003) Selective loss of spinal GABAergic or glycinergic neurons is not necessary for development of thermal hyperalgesia in the chronic constriction injury model of neuropathic pain. *Pain* 104:229–239.
- Punnakkal P, von Schoultz C, Haenraets K, Wildner H, Zeilhofer HU (2014) Morphological, biophysical and synaptic properties of glutamatergic neurons of the mouse spinal dorsal horn. *J Physiol* 592:759–776.
- Reilly JP, Freeman VT, Larkin WD (1985) Sensory effects of transient electrical stimulation—evaluation with a neuroelectric model. *IEEE Trans Biomed Eng* 32:1001–1011.
- Russo M, Cousins MJ, Brooker C, Taylor N, Boesel T, Sullivan R, Poree L, Shariati NH, Hanson E, Parker J (2018) Effective relief of pain and associated symptoms with closed-loop spinal cord stimulation system: preliminary results of the avalon study. *Neuromodulation* 21:38–47.
- Schoen I, Fromherz P (2008) Extracellular stimulation of mammalian neurons through repetitive activation of Na⁺ channels by weak capacitive currents on a silicon chip. *J Neurophysiol* 100:346–357.
- Schoffnegger D, Heinke B, Sommer C, Sandkuhler J (2006) Physiological properties of spinal lamina II GABAergic neurons in mice following peripheral nerve injury. *J Physiol* 577:869–878.
- Shealy CN, Mortimer JT, Reswick JB (1967) Electrical inhibition of pain by stimulation of the dorsal columns: preliminary clinical report. *Anesth Analg* 46:489–491.
- Shechter R, Yang F, Xu Q, Cheong YK, He SQ, Sdrulla A, Carteret AF, Wacnik PW, Dong X, Meyer RA, Raja SN, Guan Y (2013) Conventional and kilohertz-frequency spinal cord stimulation produces intensity- and frequency-dependent inhibition of mechanical hypersensitivity in a rat model of neuropathic pain. *Anesthesiology* 119:422–432.
- Smits H, van Kleef M, Joosten EA (2012) Spinal cord stimulation of dorsal columns in a rat model of neuropathic pain: evidence for a segmental spinal mechanism of pain relief. *Pain* 153:177–183.
- Song Z, Viisanen H, Meyerson BA, Pertovaara A, Linderth B (2014) Efficacy of kilohertz-frequency and conventional spinal cord stimulation in rat models of different pain conditions. *Neuromodulation* 17:226–234. discussion 234–225.
- Spike RC, Puskar Z, Andrew D, Todd AJ (2003) A quantitative and morphological study of projection neurons in lamina I of the rat lumbar spinal cord. *Eur J Neurosci* 18:2433–2448.
- Todd AJ (2010) Neuronal circuitry for pain processing in the dorsal horn. *Nat Rev Neurosci* 11:823–836.
- Todd AJ (2017) Identifying functional populations among the interneurons in laminae I–III of the spinal dorsal horn. *Mol Pain* 13. 1744806917693003.
- Yang F, Xu Q, Cheong YK, Shechter R, Sdrulla A, He SQ, Tiwari V, Dong X, Wacnik PW, Meyer R, Raja SN, Guan Y (2014) Comparison of intensity-dependent inhibition of spinal wide-dynamic range neurons by dorsal column and peripheral nerve stimulation in a rat model of neuropathic pain. *Eur J Pain* 18:978–988.
- Yasaka T, Tiong SY, Hughes DI, Riddell JS, Todd AJ (2010) Populations of inhibitory and excitatory interneurons in lamina II of the adult rat spinal dorsal horn revealed by a combined electrophysiological and anatomical approach. *Pain* 151:475–488.
- Yowtak J, Lee KY, Kim HY, Wang J, Kim HK, Chung K, Chung JM (2011) Reactive oxygen species contribute to neuropathic pain by reducing spinal GABA release. *Pain* 152:844–852.

(Received 23 July 2019, Accepted 18 December 2019)
(Available online 7 January 2020)